

Morphological evolution of beach cusps and associated swash circulation patterns

Gerhard Masselink *, Charitha B. Pattiaratchi

Centre for Water Research, University of Western Australia, WA 6907 Nedlands, Australia

Received 12 March 1997; accepted 6 October 1997

Abstract

A numerical model capable of simulating the motion of water particles on beach cusp morphology under the influence of an initial velocity and gravity is presented. The model indicates that the typical swash pattern on beach cusps is three-dimensional, with wave uprush diverging at the cusp horns resulting in concentrated backwash streams in the embayment. The degree of horn divergence is an increasing function of the parameter $\epsilon(S/\lambda)^2$, where ϵ quantifies the prominence of the beach cusps, S is the horizontal swash excursion length and λ is the cusp spacing. The numerical experiments are supplemented with detailed field measurements of beach cusp morphological change. The field data include three types of morphological response, each characterised by a particular pattern of swash circulation, that can be delineated using $\epsilon(S/\lambda)^2$. When $\epsilon(S/\lambda)^2 < 0.015$, beach cusp morphology is large and/or subdued in relation to the swash length. Swash circulation is essentially two-dimensional (oscillatory flow) and results in steepening of the beachface and infilling of the cusp embayments. For $\epsilon(S/\lambda)^2 = 0.015$ to 0.15 , wave uprush is deflected from the cusp horns and flows into the embayments where it exits in a concentrated backwash stream (horn divergent flow). The ensuing swash/backwash inequality reinforces cusp development and maintains existing cusp morphology. When $\epsilon(S/\lambda)^2 > 0.15$, beach cusps are small and/or pronounced in relation to the length of the swash. Overtopping and ponding of the cusp horn takes place and swash circulation is from the embayment to the horn (horn convergent flow). As a result, cusp horns are eroded and accretion occurs in the embayments. © 1998 Elsevier Science B.V. All rights reserved.

Keywords: beach cusps; swash; beach morphology; rhythmic morphology; beachface

1. Introduction

Beach cusps are rhythmic shoreline features formed by swash action. They are characterised by steep-gradient, seaward-pointing cusp horns and gentle-gradient, seaward-facing cusp embayments. The cusps are often regularly spaced and their spacing may range from ca. 10 cm to 40 m. Two main types of beach cusps on sandy beaches

are reported in the literature: (1) those formed by breaching of a previously deposited berm (Jefferson, 1899; Evans, 1938, 1945; Dubois, 1978; Sallenger, 1979; Kaneko, 1985); and (2) those that originate from deposition of cusp horns under net accretionary conditions (Kuenen, 1948; Russell and McIntire, 1965; Komar, 1973; Huntley and Bowen, 1978; Dean and Maurmeyer, 1980; Sato et al., 1981; Takeda and Sunamura, 1983; Holland and Holman, 1996; Masselink et al., 1997). The present study is concerned with the latter type.

Beach cusp morphology is associated with

* Corresponding author. Tel.: +61 8 9380 2687. Fax: +61 938 01015. E-mail: masselin@cwrr.uwa.edu.au

reflective beaches characterised by a steep beachface and modally low-energy swell conditions with surging breakers. The occurrence of the reflective beach type may be predicted using the dimensionless fall velocity (Gourlay, 1968):

$$\Omega = \frac{H_b}{w_s T} \quad (1)$$

where H_b is the breaker height, w_s is the sediment fall velocity and T is the wave period. Reflective beaches occur when $\Omega < 1$ (Wright and Short, 1984). A more dynamic threshold can be formulated using the surf similarity parameter (Battjes, 1974):

$$\xi = \frac{\tan \beta}{\sqrt{\frac{H_b}{L_o}}} \quad (2)$$

where $\tan \beta$ is the beachface gradient and L_o is the deep-water wave length given by $gT^2/2\pi$. Masselink et al. (1997) have shown that cusp destruction occurs when $\xi < 1.2$, whereas cusp build-up may take place when $\xi > 1.2$. The threshold proposed by Masselink et al. (1997) suggests that cusp build-up may occur both under the influence of surging and plunging breakers.

Beach cusp morphology in conjunction with incident waves affects the motion of swash on the beachface. Five swash flow patterns can be identified (Fig. 1). *Oscillatory* swash motion is the least complex of the patterns (Fig. 1a). Wave uprush and backwash are largely unaffected by the cusp morphology and display a simple up/down motion. *Horn divergent* swash motion is characterised by the deflection of the wave uprush from the horn to the centre of the embayment (Fig. 1b). The backwash is concentrated in the embayment and results in the formation of concentrated backwash streams, sometimes referred to as mini-rips (Bagnold, 1940; Russell and McIntire, 1965; Dean and Maurmeyer, 1980). *Horn convergent* swash motion occurs when the uprush enters the cusp embayment in a broad front aligned with the embayment contours (Fig. 1c). The uprush fans out onto the sides of the protruding horns and backwash is concentrated at the horns (Kuenen,

1948; Williams, 1973; Dyer, 1986). *Sweeping* swash motion occurs when waves approach the shoreline obliquely so that uprush and backwash sweep laterally across the beachface inducing significant littoral drift (Fig. 1d). Finally, the *swash jet* occurs after a strong backwash retards the incoming swash such that a large volume of water is concentrated at the base of the beachface (Eliot and Clarke, 1986). When sufficient hydraulic head is built up, the uprush will break through the diminishing backwash as a strong jet, spreading out in the embayment (Fig. 1e). The first three types of swash motion are typical of fair-weather conditions (i.e. $\Omega < 1$ and $\xi > 1.2$), whereas the latter two types occur under more energetic waves. The observations described in this paper were conducted under calm wave conditions and hence only the first three types of swash circulation will be considered.

The relationship between swash circulation and beach cusp morphology is not thoroughly understood, nor are the implications of the different types of swash flow for beach cusp development. Except for the latter two types of swash motion, which are clearly destructive, it is unclear to which extent the other three types are instrumental in maintaining cusp morphology. A consideration of the uprush/backwash inequality, however, appears to suggest that only the horn divergent type of swash flow is capable of maintaining and reinforcing existing beach cusp morphology (Bagnold, 1940; Russell and McIntire, 1965; Dean and Maurmeyer, 1980; Holland and Holman, 1996; Masselink et al., 1997). Horn divergent flow concentrates the wave uprush on the horns and channels the backwash through the embayments. The result is a steeper slope on the horns, because there is little destructive backwash to transport sediment seaward. In the embayments, the backwash is augmented by the flow from the horns resulting in milder embayment slopes.

Horn divergent swash circulation was measured in the field by Masselink and Pattiaratchi (1997) and Masselink et al. (1997) who used two runup wires to monitor swash motion on a cusp horn (at $y = +13$ m; Fig. 2A) and in a cusp embayment (at $y = -1$ m; Fig. 2A). Time series of the swash motion (Fig. 2B) clearly indicate that wave uprush

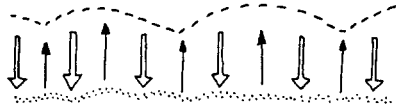
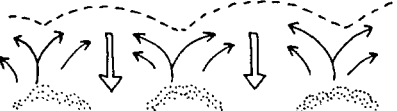
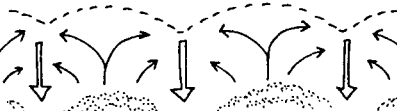
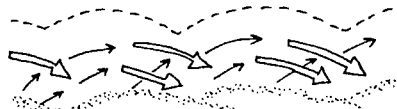
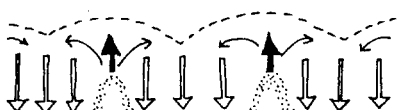
SWASH WATER CIRCULATION	DESCRIPTION
FAIR WEATHER CONDITIONS	
(a) 	OSCILLATORY <ul style="list-style-type: none"> • Predominantly two-dimensional flow up and down the beach • Weak flow divergence on cusp horns • Weak flow convergence in cusp embayments
(b) 	HORN DIVERGENT (Bagnold, 1940; Russell and McIntire, 1962; Dean and Maurmeier, 1980) <ul style="list-style-type: none"> • Swash runup is diverted from cusp horn to embayment • In the embayment, flows meet to form a concentrated backwash • Mini rips form opposite cusp embayments
(c) 	HORN CONVERGENT (Kuenen, 1948; Dyer, 1986) <ul style="list-style-type: none"> • Swash runup enters the cusp embayment with the bore front aligned with the embayment contours • Uprush spreads laterally to the horns and forms backwash • Mini rips may form opposite cusp horns
STORM CONDITIONS	
(d) 	SWEEPING <ul style="list-style-type: none"> • Swash runup sweeps obliquely across the beachface • Backwash follows a parabolic arc • Littoral drift is pronounced
(e) 	SWASH JET (Eliot and Clarke, 1986) <ul style="list-style-type: none"> • In the embayment, strong backwash retards incoming swash until it has sufficient head to overwhelm the backwash flow and rush up the beach as a narrow jet • Swash runup in the form of a swash jet fans out laterally as in (c)

Fig. 1. Types of swash flow circulation associated with beach cusp morphology.

and backwash occur several seconds earlier on the cusp horn than in the embayment. This is further illustrated by the cross-correlation function between the two swash time series (Fig. 2C) which exhibits a peak of 0.55 at a time lag of +2.5 s, indicating that maximum correspondence between the two time series occurs when the time series of embayment swash is shifted back by 2.5 s. Holland and Holman (1996) also demonstrated that swash motions in cusp embayments lag motions on the horns, in their case by 4 s. Relative frequency distributions of the position of the instantaneous shoreline show that the swash excursion length on the horn is considerably smaller than in the embay-

ment (Fig. 2E, F). On the horn, swash motion is mainly confined between $x=20$ m (lower swash limit) and $x=10$ m (upper swash limit), resulting in a maximum swash excursion of 10 m. In the embayment, the swash motion occurs from $x=20$ m to $x=5$ m, resulting in a swash length of 15 m. The shorter excursion length on the cusp horn is in accordance with the difference in gradient between horn and embayment ($\tan\beta_{\text{horn}}=0.12$ and $\tan\beta_{\text{emb}}=0.09$; Masselink et al., 1997). The spectral characteristics of horn and embayment swash are also dissimilar (Fig. 2D). The horn swash spectrum is characterised by a single incident swell peak, corresponding to the incident wave

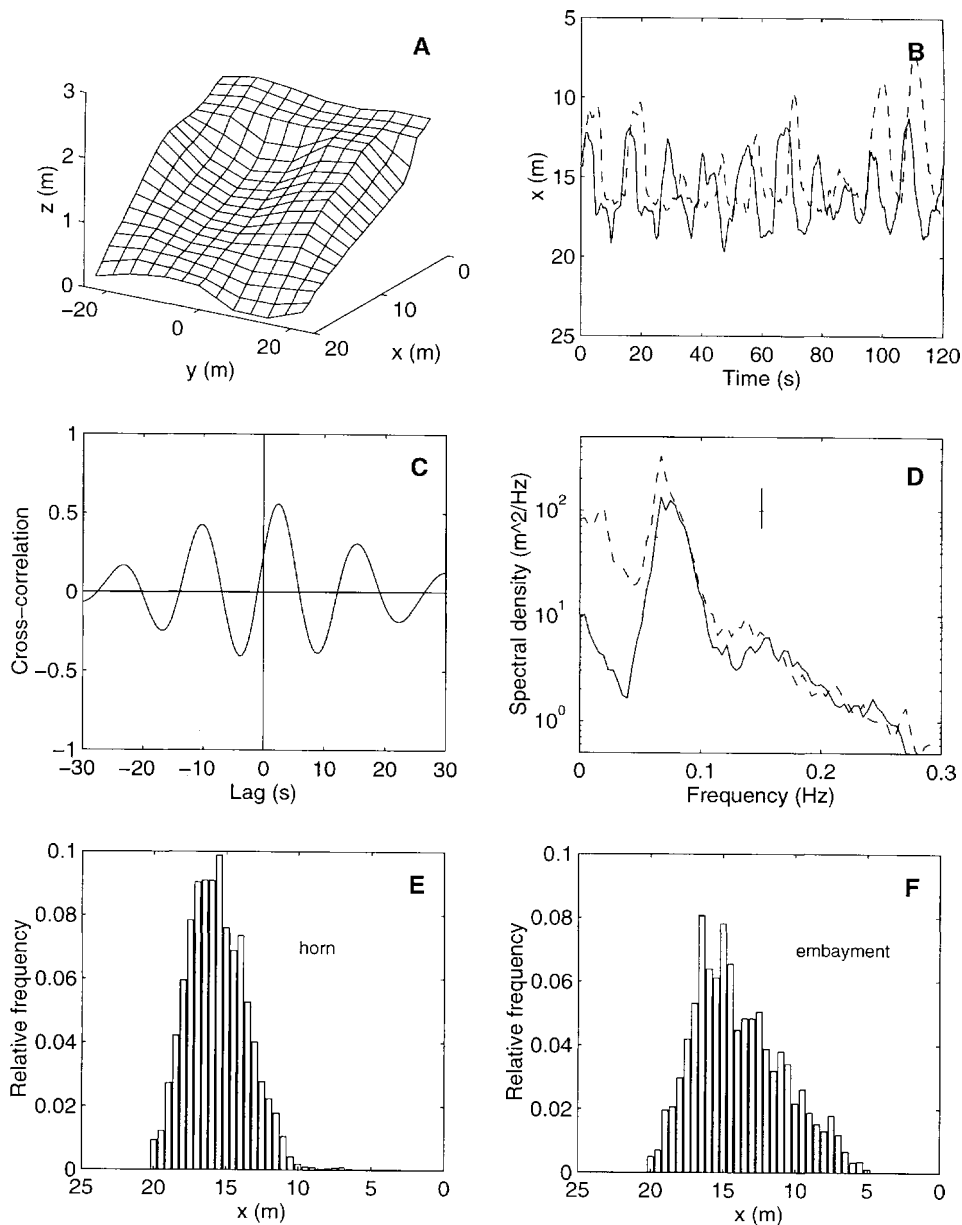


Fig. 2. (A) Beachface morphology of City Beach at 12:00 h on 7/3/95. (B) Time series of swash excursion on the cusp horn (solid line) and in the embayment (dashed line). (C) Cross-correlation between swash time series on the cusp horn and in the embayment. (D) Swash excursion spectrum of the cusp horn (solid line) and the embayment (dashed line). (E) Relative frequency distribution of swash excursion on the cusp horn. (F) Relative frequency distribution of swash excursion in the cusp embayment. Swash motion on the cusp horn was measured at $y=13$ m and in the embayment at $y=-1$ m.

peak, whereas the embayment swash spectrum contains an additional amount of energy at the low-frequency end of the spectrum. The presence

of significant amounts of low-frequency energy in the embayment swash spectrum is the result of the suppression of swash events at the base of the

beachface. Swash suppression is a common phenomenon in cusp embayments and arises because backwash volumes are usually larger than uprush volumes due to the additional swash flow from the horn. Several of such swash suppression events can be discerned in the swash time series (at $t=35$ s and $t=80$ s in Fig. 2B).

The recently proposed self-emergence model of beach cusp formation (Werner and Fink, 1993) considers horn divergent swash motion characteristic of beach cusp morphology. According to this model, beach cusps develop through feedback processes between beach morphology and three-dimensional swash flow. Positive feedback enhances existing topographic irregularities, whereas negative feedback inhibits morphological change on well-developed cusps. Werner and Fink (1993) used computer simulations to demonstrate that the cusp spacing λ is scaled by the swash excursion length S :

$$\lambda = fS \quad (3)$$

where f averages 1.7 for the simulated cusps, but ranges between 1 and 3 depending on the details of the computer algorithm. Several researchers have demonstrated that beach cusp spacing is related to the length of the swash excursion or the size of the incident waves (Johnson, 1910; Evans, 1938; Longuet-Higgins and Parkin, 1962; Williams, 1973; Dean and Maurmeyer, 1980; Sunamura, 1989). In particular, Takeda and Sunamura (1983) provides strong support for the self-emergence model by suggesting on the basis of a large number of field and laboratory measurements that the ratio of beach cusp wavelength to swash length is 1.5.

The objective of the present paper is to investigate the relation between swash circulation patterns and beach cusp morphology using a numerical model and field observations. The present field observations differ from most other field studies of beach cusps in that the morphological measurements were collected with a fine spatial (horizontal scale in metres, vertical scale in centimetres) and temporal resolution (in hours). The numerical model results are presented first to provide the theoretical framework within which the field data are to be considered.

2. Numerical model of swash circulation on beach cusp morphology

The characteristics of three-dimensional swash circulation were investigated numerically using idealised cusp morphology and simple water particle kinematics. The model presented here is similar, although a bit more sophisticated, than that of Dean and Maurmeyer (1980).

The idealised beach cusp morphology is represented by:

$$h(x, y) = x \tan \beta \left(1 + \epsilon \sin \frac{2\pi y}{\lambda} \right) \quad (4)$$

where h is the elevation of the sand surface above some datum (the lower swash limit), x is the cross-shore coordinate, y is the along-shore coordinate, $\tan \beta$ is the mean beachface gradient (averaged over the beach cusp system), ϵ is a parameter representing the prominence of the cusps and λ is the beach cusp spacing. The parameter ϵ quantifies the difference in beachface gradient between cusp horn and embayment:

$$\begin{aligned} \epsilon &= \frac{\tan \beta_{\text{horn}} - \tan \beta_{\text{emb}}}{\tan \beta_{\text{horn}} + \tan \beta_{\text{emb}}} \\ &= \frac{\tan \beta_{\text{horn}} - \tan \beta_{\text{emb}}}{2 \tan \beta} = \frac{\Delta \tan \beta}{2 \tan \beta} \end{aligned} \quad (5)$$

where $\tan \beta_{\text{horn}}$ and $\tan \beta_{\text{emb}}$ are the beachface gradients for the cusp horn and embayment, respectively, and $\Delta \tan \beta$ is defined as the difference in gradient between horn and embayment.

The water motion is defined by discrete particles subject to an initial velocity and gravitational force, neglecting the effect of friction. The governing equations for the water particles are:

$$\frac{\partial u}{\partial t} = -g \frac{\partial h}{\partial x} \quad (6)$$

$$\frac{\partial v}{\partial t} = -g \frac{\partial h}{\partial y} \quad (7)$$

where u is the cross-shore flow velocity (in the x -direction), v is the along-shore flow velocity (in the y -direction), t is time and g is gravity. For constant cross-shore and along-shore gradients,

integration of Eqs. (6) and (7) yields:

$$x_t = u_0 t - 0.5 g \tan \beta t^2 \quad (8)$$

$$y_t = v_0 t - 0.5 g \tan \gamma t^2 \quad (9)$$

where u_0 and v_0 are the initial velocities (at $t=0$) in the x - and y -direction, respectively, $\tan \beta$ is the cross-shore gradient and $\tan \gamma$ is the along-shore gradient. The swash period T_s and the swash excursion length S (position of the shoreline at $t=0.5T_s$) are easily derived from Eq. (8):

$$T_s = \frac{2u_0}{g \tan \beta} \quad (10)$$

$$S = \frac{u_0^2}{2g \tan \beta} \quad (11)$$

Note that the swash excursion is defined here in the x -direction, whereas field observations generally measure swash motion along the beachface surface. The latter is given by $u_0^2/2g \sin \beta$ which is very similar to Eq. (11) for the small beach gradients encountered in nature.

Eqs. (8) and (9) do not account for variations in the beach gradient and can therefore not be used with much confidence to track the motion of water particles on beach cusp morphology. Therefore, a finite-difference approximation of Eqs. (8) and (9) was derived:

$$x_t = x_{t-\Delta t} + u_{t-\Delta t} \Delta t - 0.5 g \tan \beta_{x_{t-\Delta t}, y_{t-\Delta t}} \Delta t^2 \quad (12)$$

$$u_t = u_{t-\Delta t} - g \tan \beta_{x_{t-\Delta t}, y_{t-\Delta t}} \Delta t \quad (13)$$

$$y_t = y_{t-\Delta t} + v_{t-\Delta t} \Delta t - 0.5 g \tan \gamma_{x_{t-\Delta t}, y_{t-\Delta t}} \Delta t^2 \quad (14)$$

$$v_t = v_{t-\Delta t} - g \tan \gamma_{x_{t-\Delta t}, y_{t-\Delta t}} \Delta t \quad (15)$$

where Δt is the time increment and the other parameters are defined above. The numerical simulations were initiated using initial velocities u_0 and v_0 (the latter was 0 m s^{-1}) and the time step used was 0.05 s .

An example of the three-dimensional swash flow computed with the water particle model is shown in Fig. 3. The simulation was conducted with an initial cross-shore velocity $u_0 = 5.5 \text{ m s}^{-1}$, a cusp spacing $\lambda = 30 \text{ m}$, a mean cross-shore gradient $\tan \beta = 0.1$ and $\epsilon = 0.1$. The average swash period and excursion for this simulation were 11 s

(Eq. (10)) and 15.4 m (Eq. (11)), respectively. The model parameters are similar to the field measurements of swash motion discussed in Section 1 (cf. Fig. 2). Divergence of the swash flow on the cusp horns and convergence in the embayments is immediately apparent (Fig. 3). Because the water particles are allowed to pass through each other uninterrupted, they can cross the centre of the embayment and run down the opposite flank of the horn from where their motion was initiated. In reality, the deflected uprush from the opposing flanks of the cusp horns meet in the centre of the embayments where they join to form concentrated backwash streams.

The extent of horn divergence can be quantified by defining a divergence parameter DP :

$$DP = \frac{\Delta y}{\lambda} \quad (16)$$

where Δy is the width of the cusp area from where the originating uprush crosses the centre line of the cusp embayment and λ is the cusp spacing. A value of $DP = 1$ indicates that all water particles entering the beach cusp system as uprush will eventually cross the centre of the embayment at some stage during swash motion. A value of $DP = 0$ indicates that not a single water particle entering the beach cusp system crosses the centre of the embayment. The model run shown in Fig. 3 is characterised by $DP = 0.74$.

The degree of horn divergence, parametrised by DP , is expected to increase with the prominence of the beach cusp and the time that a water particle is subject to the along-shore gradients associated with cusp morphology (i.e. swash period T_s). In other words, DP must be directly related to the relative distance y/λ that a water particle can travel in the along-shore direction during swash motion. The upper limit to y/λ is 0.5 , when all the water running up the cusp system will eventually cross the embayment line ($DP = 1$). The along-shore motion of water particles on beach cusp morphology is described by Eq. (9) and for $v_0 = 0 \text{ m s}^{-1}$ reduces to:

$$y = 0.5 g \tan \gamma T_s^2 \quad (17)$$

where y is the along-shore distance travelled over

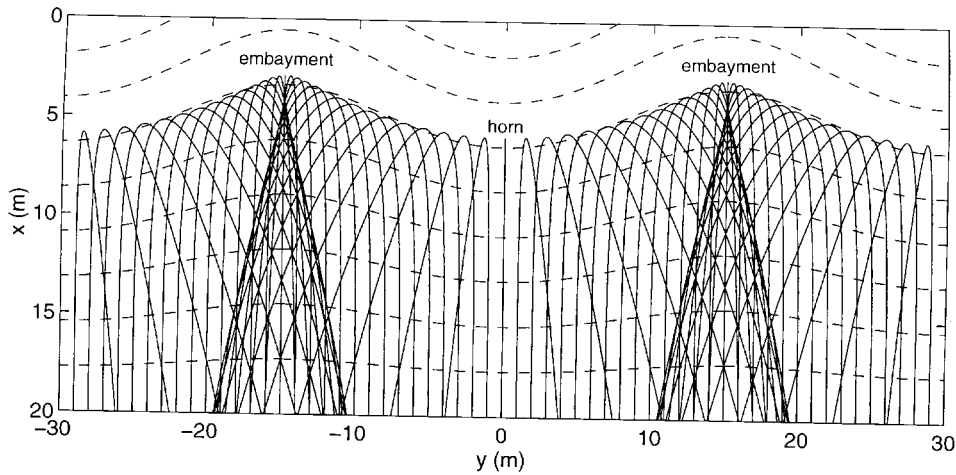


Fig. 3. Motion of water particles on idealised beach cusp morphology under the influence of an initial velocity and gravity. The dashed lines indicate elevation contours of the idealised morphology at 0.25-m intervals from 0 to 2.0 m. The labelling of the x -axis has been modified to conform to the field data (x increases in the offshore direction).

the swash period. The average along-shore gradient from horn to embayment at the maximum swash excursion is given by:

$$\tan \gamma = \frac{S \Delta \tan \beta}{0.5 \lambda} \quad (18)$$

and inserting Eq. (18) in Eq. (17) yields:

$$y = \frac{g S \Delta \tan \beta T_s^2}{\lambda} \quad (19)$$

Eq. (5) may be rewritten as:

$$\Delta \tan \beta = 2 \epsilon \tan \beta \quad (20)$$

and Eqs. (10) and (11) can be re-organised into:

$$T_s = 2 \sqrt{\frac{2S}{g \tan \beta}} \quad (21)$$

Inserting Eqs. (20) and (21) in Eq. (19) results in a relative distance y/λ of:

$$\frac{y}{\lambda} = 16 \epsilon \left(\frac{S}{\lambda} \right)^2 \quad (22)$$

where the value of the constant (16) is only approximate because the idealised cusp morphology described by Eq. (4) is characterised by a periodically varying along-shore gradient and not

by a linear gradient as assumed in the derivation of Eq. (18).

The parameter $\epsilon(S/\lambda)^2$ thus provides an appropriate scaling for the degree of horn divergence and is expected to be related to DP obtained from the numerical model. Fig. 4 plots the relation between DP and $\epsilon(S/\lambda)^2$. The different data points reflect a total of 702 model runs for different boundary conditions comprising of all the possible combinations of $\tan \beta$ (0.1–0.2 at steps of 0.05), ϵ (0.05–0.3 at steps of 0.05) and λ/S (0.5–10 at steps of 0.25). All data collapse on one line (fitted for convenience), confirming the proposed scaling is suitable. The first part of the curve is steep, indicating that small changes in $\epsilon(S/\lambda)^2$ induce large variations in DP . Beyond $\epsilon(S/\lambda)^2 = 0.05$, the curve flattens and DP becomes relatively insensitive to $\epsilon(S/\lambda)^2$. Maximum horn divergence ($DP=1$) is attained at $\epsilon(S/\lambda)^2 = 0.15$.

3. Field observations

3.1. Environmental setting

Two six-day field surveys were conducted on two beaches along the southwestern Australian

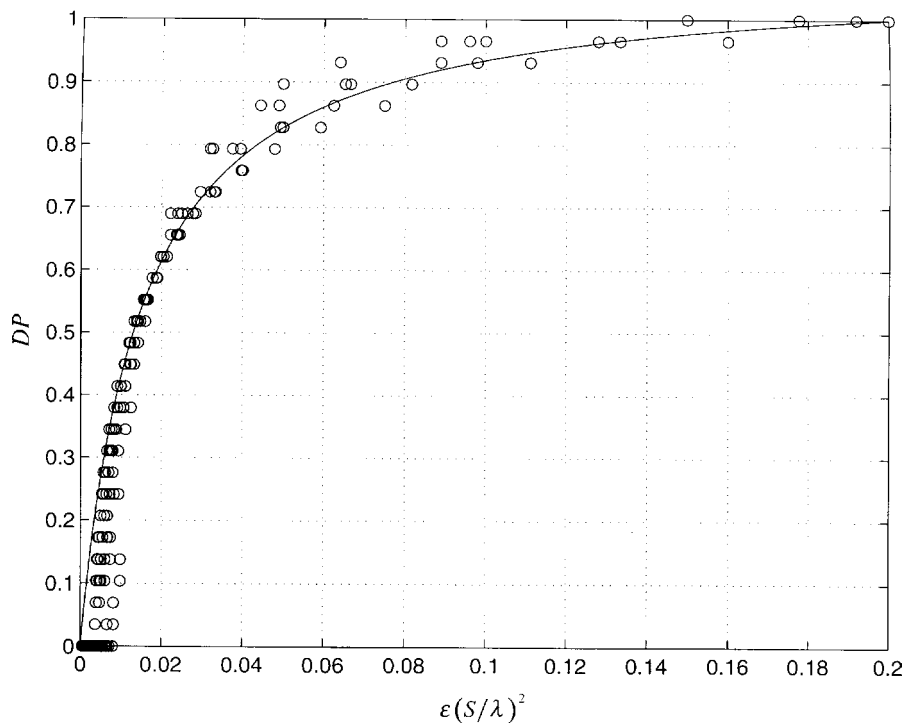


Fig. 4. Numerical results showing the relation between the horn divergence parameter DP and the scaling parameter $\epsilon(S/\lambda)^2$. The line through the numerical data has been fitted for convenience.

coastline (Fig. 5). The coast is subject to mixed, mainly diurnal, microtidal conditions with a maximum spring tide range of 0.9 m (Department of Defence, 1996). The offshore wave climate is characterised by moderate- to high-energy swell predominantly from the southwest (Silvester, 1976). However, the inshore wave conditions in front of the two selected beaches, City Beach and Myalup Beach, are moderate due to sheltering by Rottnest Island and Cape Naturaliste, respectively (Fig. 5). Beach cusp morphology is generally present on both beaches (cf. Russell and McIntire, 1965), particularly in the summer months.

3.2. Methodology

Data discussed here comprise measurements of the three-dimensional beach morphology and near-shore wave conditions, and observations of the swash circulation pattern and swash excursion length. The morphology was monitored using an

extensive array of survey pegs arranged into seven (City Beach) or nine (Myalup Beach) cross-shore transects. The transects were spaced at 7.5 m (City Beach) or 5 m intervals (Myalup Beach) and along each transect, twenty steel pegs (8 mm thick and 1 m long) were inserted in the beach at intervals of 1 m, extending from the top of the berm to the base of the beachface. The majority of the pegs were installed above mean sea level (MSL). The sand surface adjacent to the pegs was surveyed every morning, whereas the height of the pegs above the sand surface was measured hourly (City Beach) or two-hourly (Myalup Beach) using a specially designed ruler. By combining and cross-checking survey data with peg data, a continuous time series of the beachface morphology was obtained. An extensive error analysis was carried out on the City Beach data set (Feaver, 1995) and the overall accuracy of the bed elevation measurements, after removal of outliers, is considered better than ± 0.03 m. Bed elevations were transfer-

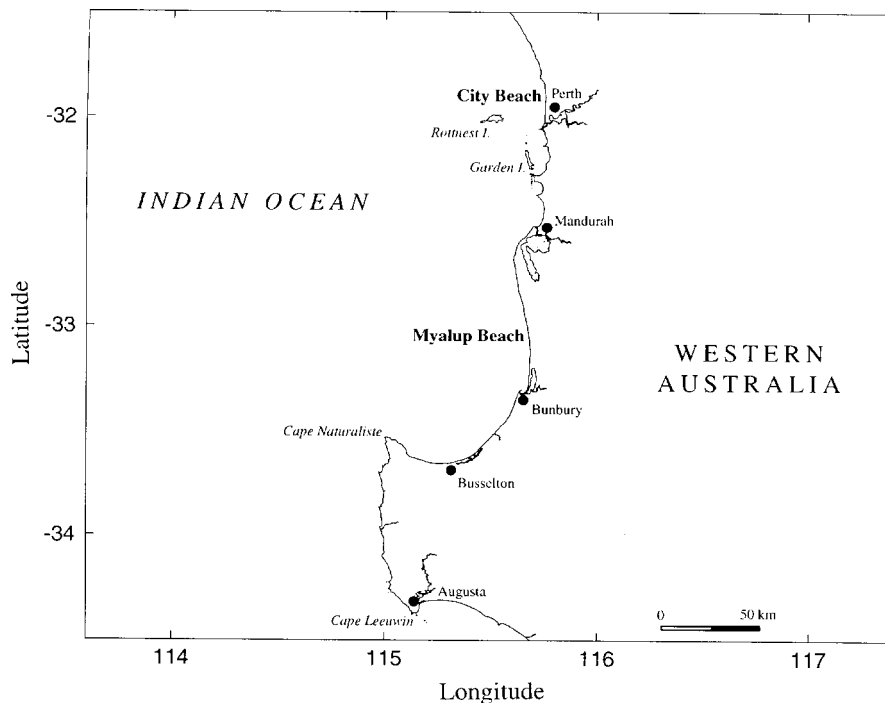


Fig. 5. Location of City and Myalup beaches in southwestern Australia.

red to MSL using the mean water depth over the survey period obtained from a pressure sensor deployed in approximately 1.5 m water depth. The pressure sensor was located outside the surf zone at all times. Additional measurements of water surface elevation and cross-shore current velocity were made 5–10 m from the shoreline in 0.5 m water depth.

Four sequences of cusp change were extracted from the two field surveys (a complete documentation of the morphological changes on City Beach is provided in Masselink et al. (1997)). These are discussed below in the order determined by the parameter $\epsilon(S/\lambda)^2$. The summary statistics for each of the sequences are given in Table 1. Pressure sensor data were used to compute the root mean square wave height H_{rms} and zero-downcrossing period T_z . The sediment size D_{50} and sediment fall velocity w_s relate to mid-beachface sediments. The mean beachface gradient $\tan\beta$ was obtained by averaging the gradients for each of the transects determined by fitting a first-order polynomial to the active part of the beachface. The difference

between horn and embayment gradient $\Delta\tan\beta$ was determined by selecting the appropriate horn and embayment transect(s) and taking the difference in gradient between the transects. The maximum swash excursion length S was estimated from the difference between the upper and lower swash level. The former was determined from a combination of field observations and inspection of the morphological change data, whereas the latter was taken as the intersection of the mean tide level with the beachface (Nielsen and Hanslow, 1991). The cusp spacing was measured using a tape measure.

There are large errors involved in estimating ϵ (ca. $\pm 30\%$) and S (ca. $\pm 20\%$), and to a lesser extent λ (ca. $\pm 5\%$). If the individual error margins of the parameters involved are combined to determine the final error margin associated with $\epsilon(S/\lambda)^2$, the extent of the uncertainty of the estimate turns out to be larger than the estimate itself (e.g. event 1 is characterised by a value at the start of the sequence of $\epsilon(S/\lambda)^2 = 0.129$, but the error range is 0.05–0.30). Such large uncertainties effec-

Table 1
Morphodynamic summary of cusp change events

H_{rms} (m)	T_z (s)	D_{50} (mm)	w_s (m/s)	$\tan\beta$	Ω	ξ	$\Delta\tan\beta_1$	$\Delta\tan\beta_2$	S_{upper} (m)	S_{lower} (m)	S (m)	λ_1 (m)	λ_2 (m)	$\epsilon_1(S/\lambda_1)^2$	$\epsilon_2(S/\lambda_2)^2$
Event 1: Horn erosion on Myalup Beach from 10:00–14:00 h on 10/2/96															
0.45	13	0.5	0.07	0.14	0.5	3.4	0.05	0.06	2	19	17	20	40	0.129	0.039
Event 2: Cusp accentuation on City Beach from 20:00 h on 6/3/95 to 14:00 h on 7/3/95															
0.3	10	0.4	0.055	0.11	0.6	2.5	0.04	0.06	7	20	13	30	30	0.034	0.051
Event 3: Embayment infilling on Myalup Beach from 8:00 h on 11/2/96 to 14:00 h on 12/2/96															
0.6	12	0.5	0.07	0.15	0.7	2.9	0.06	0	5	17	12	40	0	0.018	0
Event 4: Cusp formation on Myalup Beach from 14:00–16:00 h on 14/2/96															
0.4	11	0.5	0.07	0.18	0.5	3.9	0	0.02	6	17	11	0	20	0	0.017

H_{rms} =root mean square wave height; T_z =zero-downcrossing wave period; D_{50} =sediment size; w_s =sediment fall velocity; $\tan\beta$ =mean gradient of the active part of the beachface; Ω =dimensionless fall velocity (Eq. (1)); ξ =surf similarity parameter (Eq. (2)); $\Delta\tan\beta_1$ =difference between horn and cusp gradient at the start of the sequence; $\Delta\tan\beta_2$ =difference between horn and cusp gradient at the end of the sequence; S_{upper} =upper swash level; S_{lower} =lower swash level; S =horizontal swash excursion obtained by $S_{lower}-S_{upper}$; λ_1 =cusp spacing at the start of the sequence; λ_2 =cusp spacing at the end of the sequence.

tively render the quantitative aspects of the field measurements meaningless from a statistical point of view. However, it is felt that the sequence of $\epsilon(S/\lambda)^2$ values reported here indicate different types of swash circulation patterns and hence are of relevance, at least in a qualitative sense.

3.3. Horn erosion

Pronounced beach cusp morphology with a spacing of 20 m was present on Myalup Beach during the morning of 10/2/96 (Fig. 6). The cusp morphology consisted of alternating large and small cusp horns. Within the survey grid, large cusp horns were found at $y=-20$ m and $x=20$ m, whereas a small cusp horn was located at $y=0$ m. It was inferred that the smaller cusp horns had been deposited within larger pre-existing cusp embayments prior to the start of the field survey.

The swash circulation was dominated by two main features. Firstly, overtopping and ponding of the larger cusp horns occurred during the uprush phase of the swash, resulting in sediment deposition on the tops of these horns due to infiltration effects (e.g. Grant, 1948). This process was particularly important for the cusp horn located at $y=20$ m, and to a lesser extent for that part of the

cusp horn at $y=-20$ m that was located just outside the survey area. Secondly, swash circulation was predominantly three-dimensional from the embayment to the horn (horn convergent swash flow; Fig. 1c). The lateral swash motion ponded the smaller cusp horns from the sides and during the backwash sediment was removed from the ponded areas and transported offshore. Cusp horn 'islands' developed and ongoing erosion due to increased ponding and overtopping eventually removed these horn remnants (cf. Longuet-Higgins and Parkin, 1962; Seymour and Aubrey, 1985). At the same time, sediment deposition prevailed in the cusp embayment. Within 4 h every second horn was removed and the cusp spacing increased from 20 to 40 m. The destruction of every alternate horn was accomplished under reflective wave conditions with surging/plunging breakers ($\Omega=0.5$ and $\xi=3.4$; Table 1). The value of $\epsilon(S/\lambda)^2$ was 0.129 prior to horn destruction and 0.039 at the end of the sequence (Table 1).

Horn convergent swash circulation and overtopping of cusp horns is not reproduced by the water particle model discussed in Section 2. In fact, the model indicates the occurrence of pronounced horn divergent swash flow for $\epsilon(S/\lambda)^2=0.129$ ($DP\sim 0.95$; Fig. 4). When DP approaches a value of 1, practically all the water entering the cusp

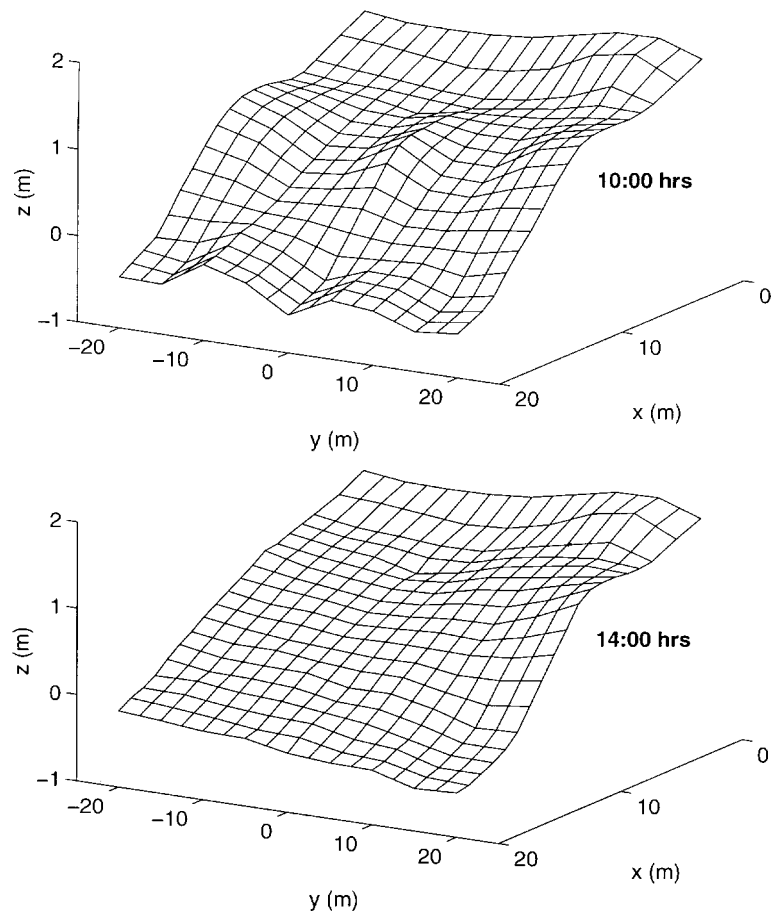


Fig. 6. Increase in cusp spacing from 20 to 40 m due to the removal of every alternate cusp horn (Myalup Beach: 10 : 00–14 : 00 h on 10/2/96).

system will exit the cusp system through the embayment. In reality, this situation can not occur because the accumulation of a large volume of water in the centre of the cusp embayment will give rise to a large hydraulic gradient from the embayment to the horns. This gradient will force water to flow from the embayment to the horn, typical of horn convergent flow. The local water pressure gradient is not considered in the present water particle model and this provides a significant shortcoming of the model.

Swash flow from the embayment to the horn was also observed by Kuenen (1948) who considered such a swash circulation pattern constructive. However, consideration of the uprush/backwash

inequality indicates that cusp morphology can not be maintained under such conditions. Spreading of the uprush within the embayment and channeling of the flow at the cusp horns must result in onshore transport and accretion within the embayment and offshore transport and erosion at the location of the cusp horn. According to Williams (1973), swash flow from the embayment to the horn is prevalent under 'gentle' swash action. Dyer (1986) denotes that gentle beachface gradients are conducive to inducing horn convergent flow. Both Williams (1973) and Dyer (1986) ascribe horn convergent flow to the effects of wave refraction, which is not accounted for in the water particle model either ($v_0 = 0$).

3.4. Cusp maintenance/accenuation

The southwestern Australian coastline is characterised by strong sea breezes in the summer (Masselink, 1996; Masselink and Pattiaratchi, 1997; Pattiaratchi et al., 1997). During sea breeze activity, small obliquely-incident wind waves become superimposed on the swell and erode the cusp horns and deposit sand in the embayments (sweeping swash motion; Fig. 1d). Consequently, the beach cusp morphology becomes more subdued. After the sea breeze ceases and the wind waves disappear, the cusp morphology is accentuated (Masselink and Pattiaratchi, 1997; Masselink et al., 1997).

Fig. 7 shows the modifications that occurred to existing beach cusp morphology on City Beach from 20:00 h on 6/3/95 to 14:00 h on 7/3/95 following sea breeze activity. The swash flow data shown in Fig. 2 were collected at the end of this 18-h morphological sequence. Sediment deposition on the horns and erosion in the embayment resulted in more pronounced beach cusp morphology. The swash circulation pattern during the cusp accentuation phase was from the horn to the embayment (horn divergent swash flow; Fig. 1b),

and reflective conditions prevailed over the entire period with surging/plunging breakers ($\Omega=0.6$ and $\xi=2.5$; Table 1). During the cusp accentuation sequence $\epsilon(S/\lambda)^2$ increased from 0.034 to 0.051 (Table 1). The water particle model indicates horn divergent flow conditions with DP increasing from 0.75 to 0.85 for $\epsilon(S/\lambda)^2$ (Fig. 4). As outlined in Section 1, the resulting uprush/backwash inequality is instrumental in maintaining and reinforcing existing cusp morphology.

3.5. Embayment infilling

After the removal of every second cusp horn on Myalup Beach on 10/2/96 (refer Section 3.3), the remaining cusp morphology was rather subdued with a spacing of 40 m. Over a period of 30 h, the cusp morphology was gradually buried from 8:00 h on 11/2/97 to 14:00 h on 12/2/97 (Fig. 8). The cusp horns retreated under the influence of onshore sediment transport, at the same time building up the berm. The cusp embayment disappeared through erosion of its subaqueous part and accretion of the subaerial part. Consequently, the gradient within the embayment became steeper. The general perception of the cusp evolution was

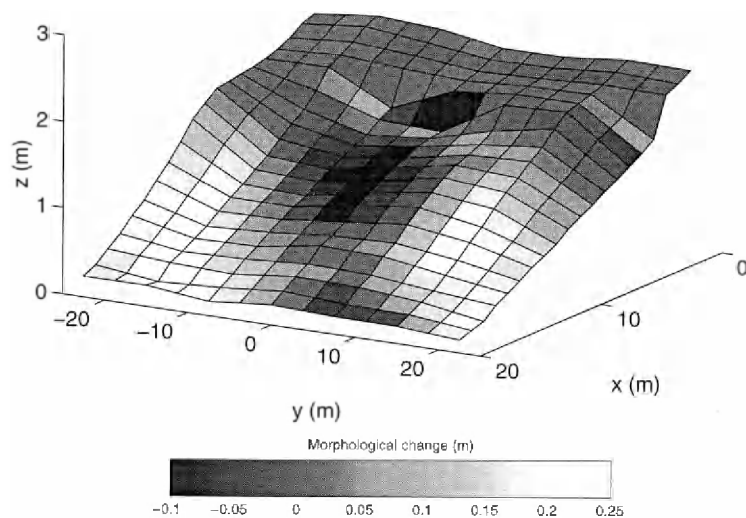


Fig. 7. Accentuation of beach cusps with a spacing of 30 m (City Beach: 20:00 h on 6/3/96 to 14:00 h on 7/3/95). The three-dimensional surface shows the beachface morphology at the start of the stated period and the shading indicates the change in sediment elevation that occurred over the period.

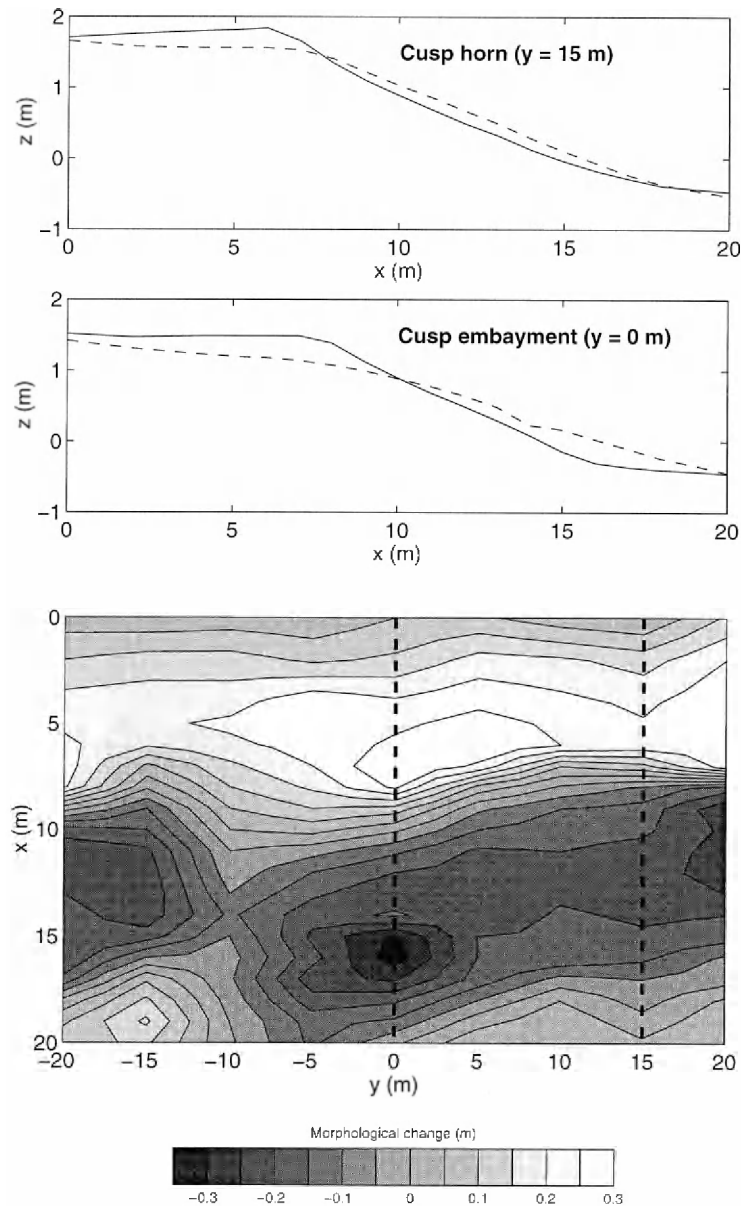


Fig. 8. Infilling of beach cusp morphology accomplished primarily through steepening of the embayment profile (Myalup Beach: 8:00 h on 11/2/96 to 14:00 h on 12/2/96).

one of infilling of the embayment and building up of a berm.

Initially, the wave uprush on the horn was deflected towards the embayment to some degree. Convergence within the embayment, however, was limited and concentrated backwash streams

were not observed. As the morphology became more subdued, flow divergence on the cusp horn was reduced even more and by the end of the period the swash motion was predominantly two-dimensional (oscillatory swash flow; Fig. 1a). Morphodynamic conditions were reflective with

surging/plunging breakers ($\Omega=0.7$ and $\xi=3.1$; Table 1). At the start of the sequence of embayment infilling $\epsilon(S/\lambda)^2$ was 0.018 (Table 1).

The water particle model indicates horn divergent swash flow for $\epsilon(S/\lambda)^2=0.018$, characterised by $DP \sim 0.55$ (Fig. 5). The value of the divergence parameter seems to suggest that deflection of the uprush from the cusp horns must have been quite pronounced. However, field observations indicated that horn divergence was rather weak and oscillatory swash flow was the prevailing mode of swash circulation. Oscillatory swash flow reduces the uprush/backwash inequality typical of horn divergent flow associated with beach cusp morphology. As a result the cusp horn gradient becomes gentler, whereas the gradient in the embayment will steepen. This process is self-reinforcing, because as the cusps become less pronounced, the flow becomes even more two-dimensional. Eventually, a straight berm results, primarily through infilling of the cusp embayment.

3.6. Beach cusp formation

Incipient formation of beach cusps was monitored on 14/2/96 on Myalup Beach (Fig. 9). At 14:00 h the beachface was planar with no along-shore rhythmicity present and oscillatory swash motion on the beachface. However, around 15:00 h, the swash flow was weakly, but distinctly three-dimensional; part of the wave uprush at $y=-5$ m was deflected to $y=-15$ m and $y=5$ m (cf. Fig. 9), resulting in increased backwash volumes and small concentrated backwash streams at the latter locations. It became apparent that the observed swash circulation pattern was actively forming beach cusps and at 16:00 h the incipient cusp morphology was very subtle, but perceivable. It also became clear at this stage that the three-dimensional swash flow was in fact horn divergent flow. Two more cusp systems formed at the same time outside the survey grid and the along-shore spacing of the rhythmic morphology was 20 m. Incipient horns (at $y=-5$ m and $y=15$ m) resulted from subaerial accretion and subaqueous erosion, causing a steepening of the beachface. Incipient embayments (at $y=-15$ and $y=5$ m) formed through subaerial erosion and subaqueous accre-

tion, thereby reducing the beachface gradient. The waves during the cusp formation were predominantly surging on the beachface and reflective conditions are indicated by the morphodynamic parameters ($\Omega=0.5$ and $\xi=3.9$; Table 1). At the end of the cusp building sequence $\epsilon(S/\lambda)^2$ was 0.017 (Table 1). Around 17:00 h the formation of the cusp morphology ceased and at 20:00 h no trace was left of the incipient cusps.

During the beach cusp formation episode described above, $\epsilon(S/\lambda)^2$ was initially zero but progressively increased during cusp development. Concomitant with the increase in $\epsilon(S/\lambda)^2$ a change in swash circulation pattern occurred from oscillatory to increasingly horn divergent. The numerical model suggests $DP \sim 0.5$ at the end of the incipient cusp formation sequence (Fig. 4).

The development of beach cusp morphology from a featureless beachface seems at odds with the finding that subdued cusps tend to disappear through the process of embayment infilling discussed in Section 3.5. Apparently, $\epsilon(S/\lambda)^2$ is not the sole factor in determining the fate of beach cusp morphology and a closer look at the hydrodynamic conditions is appropriate. Time series of water depth, wave period and spectral signature measured 20 m offshore during 14/2/96 give some suggestion as to why cusp formation started around 14:00 h and ceased around 17:00 h. The time series of the water depth (Fig. 10A) demonstrates that the incipient beach cusps were constructed under rising tide conditions. The limited time span of cusp formation therefore can not be ascribed to stationary conditions due to either high or low tide (cf. Seymour and Aubrey, 1985). The temporal variation in wave period (Fig. 10B) indicates that cusp formation occurred at the end of a phase with relative long period waves ($T > 10$ s). It is unclear why cusp formation was initiated around 14:00 h and not earlier, but the end of the cusp reconstruction clearly coincides with the wave period abruptly falling below 10 s. Inspection of the time evolution of the spectral signature is even more revealing (Fig. 10C). The figure was obtained by time-stacking successive wave spectra and contouring the resulting frequency–time plot. The spectral energy contained in the wave data

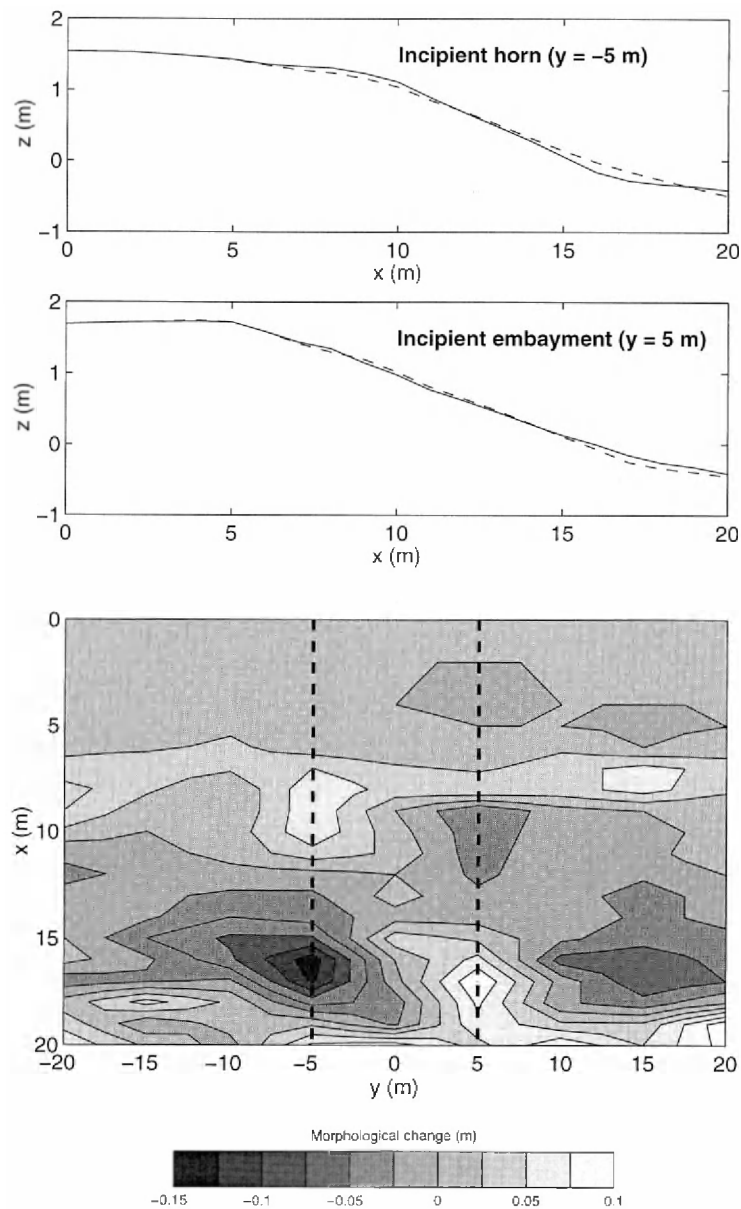


Fig. 9. Formation of incipient beach cusps with a spacing of 20 m (Myalup Beach: 14:00–16:00 h on 14/2/96).

can roughly be divided into four different frequency classes:

- (1) low-frequency energy at $f < 0.05$ Hz;
- (2) primary incident swell at $f \sim 0.08$ Hz;
- (3) first harmonic of the incident swell at $f \sim 0.16$ Hz;

- (4) wind wave energy at $f > 0.2$ Hz.

The contributions of the first two classes remained relatively constant during 14/02/96, whereas the harmonic energy decreased in importance after 15:00 h due to the rising tide level (cf. Elgar and Guza, 1985). The variation in the amount of wind

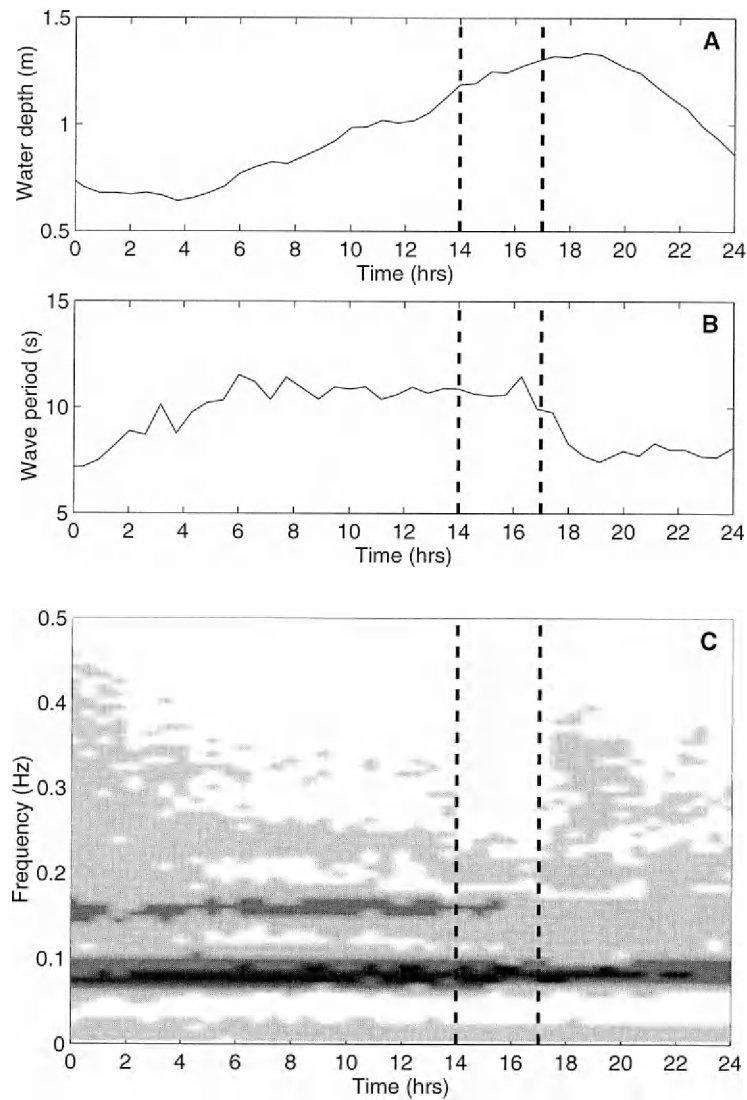


Fig. 10. Time series of: (A) water depth; (B) wave period; and (C) wave spectrum. The grey scale in (C) represents different levels of spectral density (white = $<0.005 \text{ m}^2/\text{Hz}$; light grey = $0.005\text{--}0.05 \text{ m}^2/\text{Hz}$; dark grey = $0.005\text{--}0.05 \text{ m}^2/\text{Hz}$; black = $>0.5 \text{ m}^2/\text{Hz}$). The thick dashed lines bracket the period of cusp formation (Myalup Beach: 14:00–16:00 h on 14/2/96).

wave energy implies that the period of cusp construction was characterised by the ‘cleanest’ swell, or in other words, the most narrow-banded spectrum. As confirmed by field notes, prior to and especially following cusp formation, the incident swell was superimposed by (very) small, obliquely incident wind waves ($T < 5 \text{ s}$).

4. Discussion

It would be useful to indicate threshold values for $\epsilon(S/\lambda)^2$ to delineate the different types of swash circulation pattern (horn convergent, horn divergent, oscillatory) and morphological response (horn erosion, cusp maintenance, embayment

infilling). However, the limited field data presented here do not warrant selection of threshold values. The only other data available from the literature that allow determination of $\epsilon(S/\lambda)^2$ are reported by Dean and Maurmeyer (1980). They investigated two beach cusp systems that were characterised by $\epsilon(S/\lambda)^2$ values of 0.028 (Drakes) and 0.025 (Point Reyes). These values are somewhat smaller than those reported here for cusp maintenance/accentuation ($\epsilon(S/\lambda)^2 = 0.034$ to 0.051).

Takeda and Sunamura (1983) present an extensive field data set consisting of beach cusp spacing and swash excursion length, but unfortunately ϵ was not determined. Fig. 11A shows the absolute frequency distribution of λ/S for the Takeda and Sunamura data set and indicates that beach cusp morphology is generally characterised by $\lambda/S = 1–3$. The λ/S data plotted in Fig. 11A can be converted to $\epsilon(S/\lambda)^2$ by assuming a value for ϵ . However, it is not appropriate to allocate the same value of ϵ to the wide range of λ/S values represented in the data. For example, the two beaches studied by Dean and Maurmeyer (1980) were characterised by significantly different λ/S values

(1.9 and 3.2). However, both beaches had a similar value for $\epsilon(S/\lambda)^2$ (0.028 and 0.025) because the ϵ values were different too (0.1 and 0.25). $\epsilon(S/\lambda)^2$ values were inferred for the Takeda and Sunamura data set by assuming $\epsilon = 0.15$ for $\lambda/S < 2.5$ and $\epsilon = 0.25$ for $\lambda/S > 2.5$. The resulting frequency distribution of $\epsilon(S/\lambda)^2$ is shown in Fig. 11B. The vast majority of the field observations are within the range $\epsilon(S/\lambda)^2 = 0.015–0.15$. All but one of the observations that fall outside these limits are from Longuet-Higgins and Parkin (1962) who conducted their field measurements on gravel cusps ($D_{50} = 14$ mm), unlike the other observations that were mainly made on sandy beaches.

On the basis of the present data, the measurements of Dean and Maurmeyer (1980) and the field data compiled by Takeda and Sunamura, active beach cusps are proposed to occur in a morphodynamic regime characterised by $\epsilon(S/\lambda)^2 = 0.015$ to 0.15 (Fig. 12). For these conditions, pronounced horn divergent swash flow conditions will prevail with the divergence parameter DP ranging from 0.5 to 0.95, and the cusp morphology is actively maintained or accentuated. The lower limit of $\epsilon(S/\lambda)^2 = 0.015$ marks the transition

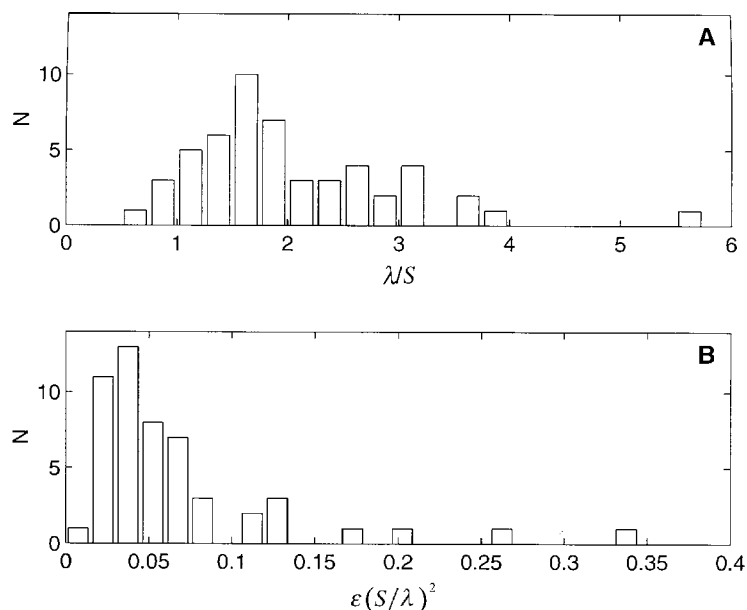


Fig. 11. Absolute frequency distribution of: (A) λ/S ; and (B) $\epsilon(S/\lambda)^2$ obtained from field measurements compiled by Takeda and Sunamura (1983).

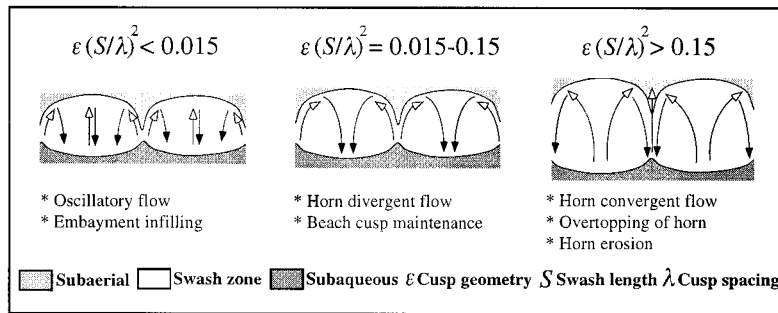


Fig. 12. Conceptual model of beach cusp morphodynamics.

to oscillatory swash circulation and consequent embayment infilling (Fig. 12). The upper limit of $\epsilon(S/\lambda)^2 = 0.15$ represents the value beyond which increased horn divergent flow conditions can not be attained because horn divergence is maximum. A number of other flow processes are dominating the swash flow including horn overtopping/ponding and horn convergent swash flow. As a consequence the cusp horns will be eroded (Fig. 12).

The relatively wide range of $\epsilon(S/\lambda)^2$ values bracketing cusp formation/maintenance inferred from this study reflects the large hydrodynamic window within which beach cusps may exist. Thus, beach cusp morphology is fairly robust and cusp spacing does not casually adjust to changing wave conditions. This is in line with Seymour and Aubrey (1985), who concluded that once a cusp spacing has been incised into the beach, it will dominate the mean spacing until a wave event occurs that establishes a radically different spacing, storm waves destroy the system entirely, or the beach cusps are completely filled in by cross-shore or along-shore sand transport. In this respect the relation between DP and $\epsilon(S/\lambda)^2$ shown in Fig. 4 is of interest. An evolving beach cusp morphology would progress along the path displayed by the numerical data. Horn divergence would initially increase rapidly (steep section of the curve in Fig. 4) even though the morphological change can be relatively minor. When the swash flow attains a certain level of horn divergence (flat section of the curve in Fig. 4) the circulation pattern is relatively insensitive to the hydrodynamic conditions. The latter can vary quite a lot without

causing a pronounced change in DP . It is probable that the beach cusps continue to involve under conditions that would not have initiated cusp formation on a planar beachface.

The present study does not provide evidence that the self-emergence theory of cusp formation is valid. Cusp morphological change and maintenance may be related to the swash flow circulation pattern, but this does not explain the actual formation of beach cusps. The self-emergence theory considers that random perturbations on the beachface eventually organise themselves into beach cusps through feedback processes between beachface morphology and swash processes (Werner and Fink, 1993). It was observed that subtle, but distinct, horn divergent swash circulation occurred when the elevation difference between incipient cusp horns and embayments was only of the order of several cm's. This is similar to the resolution of the morphological measurements reported here. To investigate whether random perturbations are a precursor to incipient cusp formation requires morphological monitoring with a resolution that is perhaps beyond what can be achieved in the field.

The field observations on Myalup Beach on 14/2/96 suggest that the initial stage of cusp formation requires a very narrow-banded and non-variable incident wave spectrum. The addition of small, obliquely incident wind waves to the existing swell was sufficient to halt the cusp formation process. Cusp formation probably may have other requirements as well, such as for example the near-correspondence of swash period and incident wave period (Bagnold, 1940; Dean and Maurmeyer,

1980). The possibility that edge wave activity, generally assumed to be responsible for beach cusps (Guza and Inman, 1975; Huntley and Bowen, 1978; Sallenger, 1979; Guza and Bowen, 1981; Inman and Guza, 1982; Seymour and Aubrey, 1985; and many others), may have played a role was also explored. Wave and current spectra collected within 10 m from the shoreline between the developing cusp horn and embayment did not reveal significant amounts of sub-harmonic energy during or just prior to cusp formation (not shown). However, this does not automatically imply that edge waves were not active; analysis of the along-shore structure of the swash motion is required to confidently disprove the presence of (standing) edge waves (Holland and Holman, 1996).

The $\epsilon(S/\lambda)^2$ thresholds proposed here to separate different swash circulation patterns and sequences of beach cusp evolution are tentative and depend strongly on how the swash length S is defined. The definition used here compares closely to the maximum excursion length, corresponding to the difference between the swash limit and the intersection of the mean sea level with the beachface. However, when a statistical estimate is used, such as the significant or root mean square swash excursion, the threshold values for $\epsilon(S/\lambda)^2$ are expected to be smaller. It should also be noted that the parameter ϵ is based on planar cross-shore profiles, whereas in reality cusp horns and embayments have distinctly convex and concave profile shapes, respectively. Derivation of the beach gradient of a non-planar profile is strongly dependent on which part of the profile is selected.

The practical difficulties in defining and measuring the relevant parameters to compute $\epsilon(S/\lambda)^2$ are, however, minor in comparison to several other limitations to the present study. Firstly, the classification of the types of flow circulation is highly subjective. Although the divergence parameter DP from the numerical model is quite useful, a quantification of the swash flow in the field is lacking. What is clearly required is the measurement of the three-dimensional flow structure of the swash in conjunction with morphological measurements. Cross-correlation between swash action on the cusp horn and in the embayment may serve as a first-order approximation of the nature of the

three-dimensional swash circulation (cf. Fig. 2C), but more rigorous data collection and analysis techniques such as reported by Holland and Holman (1996) are desirable. Secondly, only four sequences of cusp morphological change are reported here and additional observations are necessary to substantiate and validate the ideas presented here. Such observations are not necessarily involved: ϵ is easily obtained from a survey of cusp horn and embayment, S can be estimated from observing the swash excursion of a large number of swashes (~ 100) and λ can be measured with a tape measure. Thirdly, the water particle model discussed in Section 2 does not include the effects of local water gradients and refraction on the swash circulation. The idealised cusp morphology used in the model neither allows for overtopping of the cusp horn. Further numerical modeling, along the lines of the model of Werner and Fink (1993), should be carried out to improve our understanding of the relation between swash flow and cusp morphology.

5. Conclusions

A numerical model capable of simulating the motion of water particles on beach cusp morphology was combined with detailed field measurements of beach cusp morphological change to investigate the relation between swash circulation and beachface morphology. Three types of swash circulation patterns, each associated with a characteristic cusp morphological response, were identified. The occurrence of the different swash patterns was related to $\epsilon(S/\lambda)^2$, where ϵ describes the geometry of the beach cusps (cf. Eq. (5)), S is the maximum swash excursion length and λ is the cusp spacing. $\epsilon(S/\lambda)^2$ essentially parameterises the relative along-shore distance y/λ that a water particle can travel during one swash cycle under the influence of the lateral gradient associated with beach cusp morphology.

A conceptual model of beach cusp morphodynamics, whereby the parameter $\epsilon(S/\lambda)^2$ is related to the swash circulation pattern and cusp morphological evolution, is proposed (Fig. 12):

When $\epsilon(S/\lambda)^2 < 0.015$, the beach cusp morphol-

ogy is too widely spaced or too subdued relative to the swash excursion. Swash circulation is essentially two-dimensional (oscillatory) and eventually results in the infilling of the embayments.

For intermediate values of $\epsilon(S/\lambda)^2 = 0.015$ to 0.15, the cusp system is 'in tune' with the swash flow and the swash circulation is from the horn to the embayment (horn divergent). The resulting uprush/backwash inequality will result in the maintenance or accentuation of existing beach cusps.

When $\epsilon(S/\lambda)^2 > 0.15$, the beach cusp morphology is too closely spaced or too pronounced relative to the swash excursion. Field observations indicate that ponding and overtopping of the cusp horn frequently occurs, and that the swash flow is generally from the embayment to the horn (horn convergent). This causes erosion of the cusp horns and sediment accretion in the embayments. Destruction of the cusp morphology through horn convergent swash flow and overtopping is generally a rapid process, whereas infilling of the embayment through oscillatory swash motion is considerably slower.

The conceptual model needs to be validated and refined using further numerical and experimental investigations.

Acknowledgements

We would like to thank Bruce Hegge, Michael Hughes, Sheree Feaver and Dave Mitchell for their varying roles in the collection of the field data, and Ian Eliot for contributing Fig. 1 to this paper. Significant improvements to the original manuscript were suggested by an anonymous referee. This publication has Centre for Water Research reference number ED1168GM.

References

- Bagnold, R.A., 1940. Beach formation by waves: some model experiments in a wave tank. *J. Inst. Civ. Eng.* 15, 27–52.
- Battjes, J.A., 1974. Surf similarity. *Proc. 14th Int. Conf. Coastal Engineering*, ASCE, pp. 466–480.
- Dean, R.G., Maurmeyer, E.M., 1980. Beach cusps at Point Reyes and Drakes Bay beaches, California. *Proc. 17th Int. Conf. Coastal Engineering*, ASCE, pp. 863–884.
- Department of Defence, 1996. Australian National Tide Table 1990. Australian Hydrographic Publication 11, Canberra.
- Dubois, R.N., 1978. Beach topography and beach cusps. *Geol. Soc. Am. Bull.* 89, 1133–1139.
- Dyer, K.R., 1986. *Coastal and Estuarine Sediment Dynamics*, Wiley and Sons, Chichester.
- Elgar, S., Guza, R.T., 1985. Observations of bispectra of shoaling surface gravity waves. *J. Fluid Mech.* 161, 425–448.
- Eliot, I.G., Clarke, D.J., 1986. Minor storm impact on the beachface of a sheltered sandy beach. *Mar. Geol.* 73, 61–83.
- Evans, O.F., 1938. Classification and origin of beach cusps. *J. Geol.* 46, 615–627.
- Evans, O.F., 1945. Further observations on the origin of beach cusps. *J. Geol.* 53, 403–404.
- Feaver, S., 1995. The Effect of the Sea Breeze on Coastal Processes. Honours Thesis, Department of Environmental Engineering, University of Western Australia (unpubl.).
- Gourlay, M.R., 1968. Beach and Dune Erosion Tests. Report No. M935/M936, Delft Hydraulics Laboratory.
- Grant, U.S., 1948. Influence of the water table on beach aggradation and degradation. *J. Mar. Res.* 7, 655–660.
- Guza, R.T., Bowen, A.J., 1981. On the amplitude of beach cusps. *J. Geophys. Res.* 86, 4125–4132.
- Guza, R.T., Inman, D.L., 1975. Edge waves and beach cusps. *J. Geophys. Res.* 80, 2997–3012.
- Holland, K.T., Holman, R.A., 1996. Field observations of beach cusps and swash motions. *Mar. Geol.* 134, 77–93.
- Huntley, D.A., Bowen, A.J., 1978. Beach cusps and edge waves. *Proc. 16th Int. Conf. Coastal Engineering*, ASCE, pp. 1378–1393.
- Inman, D.L., Guza, R.T., 1982. The origin of swash cusps on beaches. *Mar. Geol.* 49, 133–148.
- Jefferson, M.S.W., 1899. Beach cusps. *J. Geol.* 7, 237–246.
- Johnson, D.W., 1910. Beach cusps. *Geol. Soc. Am. Bull.* 21, 599–624.
- Kaneko, A., 1985. Formation of beach cusps in a wave tank. *Coastal Eng.* 8, 81–90.
- Komar, P.D., 1973. Observations of beach cusps at Mono Lake, California. *Geol. Soc. Am. Bull.* 84, 3593–3600.
- Kuenen, P.H., 1948. The formation of beach cusps. *J. Geol.* 56, 34–40.
- Longuet-Higgins, M.S., Parkin, D.W., 1962. Sea waves and beach cusps. *Geogr. J.* 128, 194–201.
- Masselink, G., 1996. Sea breeze activity and its effect on coastal processes near Perth, Western Australia. *J. R. Soc. W. Aust.* 79, 199–205.
- Masselink, G., Pattiaratchi, C.B., 1997. Morphodynamic impact of sea breeze on a beach with beach cusp morphology. *J. Coastal Res.* 22, 1139–1156.
- Masselink, G., Hegge, B.J., Pattiaratchi, C.B., 1997. Beach cusp morphodynamics. *Earth Surf. Process. Landforms* (in press).
- Nielsen, P., Hanslow, D.J., 1991. Wave runup distributions on natural beaches. *J. Coastal Res.* 7, 1139–1152.
- Pattiaratchi, C.P., Hegge, B.J., Gould, J., Eliot, I.G., 1997. Impact of sea breeze activity on nearshore and foreshore

- processes in southwestern Australia. *Continental Shelf Res.* 17, 1539–1560.
- Russell, R.J., McIntire, W.G., 1965. Beach cusps. *Geol. Soc. Am. Bull.* 76, 307–320.
- Sallenger, A.H., 1979. Beach cusp formation. *Mar. Geol.* 29, 23–37.
- Sato, M., Kuroki, K., Shinohara, T., 1981. Field experiments of beach cusp formation. *Memoir 36th Annual Convention, Japan Society of Civil Engineers*, II, pp. 841–842 (quoted in Sunamura, 1989).
- Seymour, R.J., Aubrey, D.G., 1985. Rhythmic beach cusp formation: a conceptual synthesis. *Mar. Geol.* 65, 289–304.
- Silvester, R.A., 1976. Wanneroo Coastline. Report for the Shire of Wanneroo, Department of Civil of Engineering, University of Western Australia.
- Sunamura, T., 1989. Sandy beach geomorphology elucidated by laboratory modelling. In: Lathan, V.C., Trenhaile, A.S. (Eds.), *Applications in Coastal Modeling*. Elsevier, Amsterdam, pp. 159–213.
- Takeda, I., Sunamura, T., 1983. Formation and spacing of beach cusps. *Coastal Eng. Jpn.* 26, 121–135.
- Werner, B.T., Fink, T.M., 1993. Beach cusps as self-organized patterns. *Science* 260, 968–970.
- Williams, A.T., 1973. The problem of beach cusp development. *J. Sediment. Petrol.* 43, 857–866.
- Wright, L.D., Short, A.D., 1984. Morphodynamic variability of surf zones and beaches: a synthesis. *Mar. Geol.* 56, 93–118.